Green investment and asset stranding under transition scenario uncertainty*

Maria Flora
CREST, CNRS, IP Paris

Peter Tankov
ENSAE, IP Paris

January 11, 2022

Abstract

We develop a real-options approach to evaluate energy assets and potential investment projects under transition scenario uncertainty. Dynamic scenario uncertainty is modelled by assuming that the economic agent acquires the information about the scenario progressively by observing a signal. The problem of valuing an investment is formulated as an American option pricing problem, where the optimal exercise time corresponds to the time of entering into a potential investment project or the time of selling a potentially stranded asset. To illustrate our approach, we apply representative scenarios from different integrated assessment models to the examples of a coal-fired power plant without Carbon Capture and Storage (CCS) and potential investment into a biomass power plant with CCS.

Keywords: Transition risk, scenario uncertainty, Bayesian learning, stranded asset, real options.

1 Introduction

As the global climate is changing, the need for a major decarbonisation of the energy system has become evident [Teske, 2019, Bogdanov et al., 2019], while climate change impacts are expected throughout the energy system itself [Stanton et al., 2016, Cronin et al., 2018]. In this context, traditional risk management approaches may no longer be sufficient to evaluate energy-related assets and investment projects. While there is little doubt that the low-carbon transition will lead to profound changes in the energy system in the years and decades to come, it is difficult to predict the exact nature of these changes and the pace of the transition. Faced with such uncertainty, the scenario approach has emerged as a means to provide decision-makers with the tools to optimise their actions. Produced with the help of integrated assessment models, transition scenarios are published by international bodies such as the IEA (International Energy Agency), IPCC (International Panel on Climate Change), NGFS (Network for Greening the Financial System), IIASA (International Institute for Applied System Analysis), and used by the economic agents to understand the possible futures they need to prepare for. In particular, the NGFS maintains a database of six transition scenarios[1], described in detail in Section 3. These scenarios are used by central banks to conduct

*This research was supported by ADEME (Agency for Ecological Transition) in the context of SECRAET project, and by the FIME (Finance for Energy Markets) research initiative of the Institut Europlace de Finance.

[1]Release 2, available at `https://data.ene.iiasa.ac.at/ngfs/`

climate stress testing exercises: for example, by comparing the value of a bank's portfolio under orderly and disorderly transition scenario, one may evaluate the risk of disorderly transition.

The scenario approach, however, suffers from a number of drawbacks from the point of view of risk management and asset pricing. In most existing approaches the scenario is assumed to be given and known to the agent, thus the influence of agent's actions on the scenario, and the imperfect knowledge of the scenario by the agent are not taken into account. Yet, owners of energy assets with a risk of stranding, or of construction permits for green energy projects, make their decisions to sell the asset, or to build the plant, without the perfect knowledge of the scenario to come. Instead, they evaluate the prospects of a given asset / investment based on partial information about the state of the energy transition.

In this paper we therefore extend the real options (RO) approach to take into account (i) the transition scenario uncertainty and (ii) the progressive discovery of information about the transition scenario by the investors. Traditional RO theory already acknowledges the value of waiting and postponing the investment decision in favor of flexibility and in view of acquiring more information on the evolution of the underlying stochastic variables that the project value depends on. However, the sources of uncertainty in a RO model usually stem from the evolution of asset prices or cost variables specific to the project. We consider an additional layer of uncertainty, that is the uncertainty stemming from the energy transition scenario, potentially affecting the distribution of all stochastic variables that the value of the project depends on. Then, we introduce an active Bayesian learning component to this framework. Namely, the agents continuously update their beliefs regarding the likelihood of being in a certain climate scenario, and evaluate the projects accordingly.

Our paper contributes to different strands of literature. The literature on RO in the context of energy project valuation is vast. Indeed, RO is a prominent approach to evaluate capital investments under uncertainty and irreversibility, and energy projects provide a natural field of application given their relatively high capital costs and their multiple sources of uncertainty relative to commodity prices and future electricity demand and supply. [Siddiqui and Fleten, 2010] evaluate how a firm may proceed with staged commercialisation and deployment of competing alternative energy technologies, and find that the option of investing in such projects increases the value of the firm. [Fuss et al., 2012] analyze the impact of uncertainty for deriving the optimal portfolio of energy technologies for a profit-maximizing investor. [Boomsma et al., 2012] analyze investment decisions in renewable energy under policy interventions, and find that a feed-in tariff leads to earlier investment. [Abadie et al., 2011] employ a binomial lattice model to compute the value of the option to abandon a coal-fired power plant; [Laurikka and Koljonen, 2006] analyze how the uncertainty related to an emission trading scheme affects the value of an option to invest in a coal power plant; [Flora and Vargiolu, 2020] use a least-squares Monte Carlo approach to solve the optimization problem of decision making in case of a power producer who is considering switching from a carbon-intensive technology to a renewable one under a carbon price floor; [Hach and Spinler, 2016] assess the effectiveness of capacity payments in promoting gas-fired generation investments under different degrees of feed-in tariff. [Detemple and Kitapbayev, 2020] develop a real options model where a firm seeking to build a new power plant has the exclusive choice between two technologies, namely wind and gas.

A related literature is also that of climate-related stranded assets. [McGlade and Ekins, 2015] employ an IAM and find that a third of oil reserves, half of gas reserves and over 80 per cent of current coal reserves must remain underground to maintain the global temperature rise compared to pre-industrial level below 2°C. A more recent study [Welsby et al., 2021] finds that the 1.5°C sce-

nario requires nearly 60 per cent of oil and fossil methane gas, and 90 per cent of coal to remain unextracted. [Mercure et al., 2018] estimate, with an integrated global economy-environment simulation model, the discounted global wealth loss from stranded fossil fuel assets. [Rozenberg et al., 2020] analyze the impact of alternative policy instruments on costs and dynamics of transition from polluting to clean capital, and study their implications for asset stranding. [van der Ploeg and Rezai, 2020] study the determinants of asset stranding in the fossil-fuel industry. [Mo et al., 2021] focus on the case of China, and show that carbon pricing increases the risk for newly-built coal power plants to become stranded.

Finally, our paper also relates to the literature on active learning. In this context, closest to our paper is [Dalby et al., 2018]. They study policy uncertainty in the form of an unexpected downward adjustment of a fixed feed-in tariff (FIT) scheme, with a learning perspective. Their agent expects an adverse transition between two regimes of fixed FIT, and has the option to invest in a green energy project. Our work differs in multiple respects. First, their model pertains to renewable energy policy uncertainty rather than broader transition scenario uncertainty. Second, it is specific to renewable energy (RE) project valuation, while we develop a flexible approach that can be used for several potential applications in decision making analysis. Third, they consider a single policy revision, with two possible regimes: either the change in the FIT payment has not yet occurred (this is the starting point), or it has occurred, and in such a case the value of the option to invest in the green energy project becomes zero. In contrast, our model can include several different scenarios, and climate uncertainty shapes the trajectories of all state variables.

The paper is structured as follows. In Section 2, we present our model of an agent learning from a climate-related signal about the likelihood of the global climate scenario, and using her belief for the purpose of decision-making analysis. In Section 3, we describe an empirical application of our approach, and analyze the sensitivity of our results to a set of parameters. Section 4 concludes.

2 Model and scenario uncertainty with Bayesian learning

How can a microeconomic agent, wishing to price an asset or determine an optimal investment strategy, use a macroeconomic scenario? The macroeconomic scenarios will give the agent a sense of the magnitude of the uncertainty relative to the economic variables that are important in the agent's decision making process. Based on the arrival of exogenous signals, the profit maximizing agent will then update her subjective belief about the likelihood of being in one scenario or another. We model this processing of new information and active updating of belief in a Bayesian learning setting.

2.1 Description of the model

We consider a discrete time model, where the integer-valued variable t denotes time measured in years. In the context of long-term investment/divestment decisions, it seems reasonable to assume that the agent may revise her investment/divestment strategy once a year. A risk-neutral and profit-maximizing economic agent (owner of a power-generating asset or of the potential investment project), facing both revenue risk and scenario uncertainty, has the option to either sell the asset or to invest into the project at a future date τ. The revenues of the asset prior to closure / of the project after investment are determined by future values of risk factors (fuel prices, electricity price, carbon price) whose evolution is stochastic and whose distribution depends on the realized transition scenario. We assume there are N scenarios corresponding to different climate, economic and policy

assumptions. The true scenario is not known to the agent ex ante, however, the agent observes a signal (e.g., global CO2 emissions), which contains noisy information about the scenario, and allows the agent to progressively update her posterior probability of realization for each scenario. For example, if the emissions decrease at a steady rate, the agent will assume that an orderly transition scenario is more likely than a delayed transition scenario.

Under each scenario, consider a number K of stochastic risk factors. We assume that the value $P_{k,t}$ of the risk factor k at time t under the scenario i follows an autoregressive dynamics with scenario-dependent mean $\mu^i_{k,t}$. To write the risk factor dynamics in matrix form, we denote by $\mathbf{P}_t$ the K-dimensional vector of risk factors, by $\boldsymbol{\mu}^i_t$ the vector of drifts, by $\boldsymbol{\Phi}$ the $(K \times K)$ matrix of mean reversion rates, and by $\boldsymbol{\sigma}$ the Cholesky decomposition of the instantaneous variance-covariance matrix of the risk factors. Thus, in matrix form we have

$$\mathbf{P}_t = \boldsymbol{\mu}^i_t + \boldsymbol{\Phi}\left(\mathbf{P}_{t-1} - \boldsymbol{\mu}^i_{t-1}\right) + \boldsymbol{\sigma}\boldsymbol{\varepsilon}_t \tag{1}$$

under scenario i, where $(\boldsymbol{\varepsilon}_t)$ is a sequence of i.i.d. K-dimensional standard normal vectors.

2.2 Bayesian updates

As mentioned above, the agent does not know the true scenario i, but observes a noisy signal y_t, and infers the likelihood of being in scenario i based on this signal. Ideally, the signal should be a (scenario-dependent) variable that is highly affected by or that has a high correlation with the scenario. Thus, the signal will "reveal" to the agent, with error, the state i. For example, the signal the agent relies on could be the price of carbon in the region where the production asset is located or the agent plans to invest; or the total emissions of greenhouse gases. Let us assume the signal is normally distributed with mean $\mu^i_{y,t}$ and standard deviation σ_y, that is

$$y_t = \mu^i_{y,t} + \sigma_y \eta_t\,, \qquad \text{with} \quad \eta_t \sim N(0,1) \text{ i.i.d.} \tag{2}$$

We assume that, given the scenario, the signal is independent from the risk factors, or, in other words, η_t is independent from ε^k_t for all k. At every time step, the agent updates her prior knowledge of the state to obtain a posterior probability of each state i. For simplicity, we assume that the updates are only based on the value of the signal, but not on the values of the risk factors P_t.

The probability π^i_t of being in scenario i at time t based on the signal y_t is

$$\pi^i_t = \mathbb{P}[I = i|\mathcal{F}_t], \quad \mathcal{F}_t = \sigma(y_s, s \le t)\,, \tag{3}$$

where $\{\mathcal{F}_t : t \ge 0\}$ is the filtration generated by the observable process $\{y_t : t \ge 0\}$. In particular, the Bayesian update of π^i_t at each time step t is

$$\pi^i_t = \mathbb{P}[I = i|y_t, \mathcal{F}_{t-1}] = \frac{\mathbb{P}[I = i, y_t \in dy|\mathcal{F}_{t-1}]}{\mathbb{P}[y_t \in dy|\mathcal{F}_{t-1}]} = \pi^i_{t-1}\frac{\mathbb{P}[y_t \in dy|I = i, \mathcal{F}_{t-1}]}{\mathbb{P}[y_t \in dy|\mathcal{F}_{t-1}]}\,, \tag{4}$$

where we use the notation $\mathbb{P}[y_t \in dy|\mathcal{F}_{t-1}]$ as a short-hand for the density of y_t given $\mathcal{F}_{t-1}$, and similarly for other notation in the above equation.

The *unnormalized posterior probability* of being in scenario i is then given by

$$\hat{\pi}^i_t = \hat{\pi}^i_{t-1} e^{-\frac{\left(y_t - \mu^i_{y,t}\right)^2}{2\sigma^2_y}}\,, \tag{5}$$

and the normalized probability is

$$\pi_t^i = \frac{\hat{\pi}_t^i}{\sum_i \hat{\pi}_t^i}\,. \tag{6}$$

Provided that the scenarios offer a range of sufficiently diversified trends $\mu_{y,t}^i$ for the signal, the lower the standard deviation of the signal σ_y, the sooner the agent's belief on the likelihood of being in a certain scenario i will converge to either 0 or 1.

In real option theory, the decision making analysis of the agent is similar to the pricing of an American option. The value function (value of the asset) at date t is related, through the dynamic programming principle, to the value function at date $t+1$, and computed by backward induction. This approach relies on the specification of a dynamics for the underlying stochastic processes, that is, we need to determine the joint dynamics of the risk factors, the signal, and the scenario probabilities π_t^i, or, in other words, the rule of updating P_t, y_t and π_t^i from P_{t-1}, y_{t-1} and π_{t-1}^i. This update rule reduces to a two-step procedure:

- Simulate y_t and P_t from P_{t-1}, y_{t-1} and π_{t-1}^i.
- Update π_t^i from y_t and π_{t-1}^i.

The second update step is given by Equations (5-6). For the first simulation step, using the conditional independence of the signal and the risk factors, we compute the conditional law of P_t and y_t given $\mathcal{F}_{t-1}$:

$$\begin{aligned}\mathbb{P}[\mathbf{P}_t \in A, y_t \in B|\mathcal{F}_{t-1}] &= \sum_i \pi_{t-1}^i \mathbb{P}\left[\mathbf{P}_t \in A,\, y_t \in B|I=i\right] \\ &= \sum_i \pi_{t-1}^i \mathbb{P}\left[\mathbf{P}_t \in A|I=i\right]\mathbb{P}\left[y_t \in B|I=i\right]\,,\end{aligned} \tag{7}$$

where

$$\mathbb{P}\left[\mathbf{P}_t \in A|I=i\right] = \frac{1}{\sqrt{|\boldsymbol{\Sigma}|(2\pi)^K}}\int_A e^{-\frac{1}{2}\left(z-\boldsymbol{\Phi}\mathbf{P}_{t-1}-\left(\boldsymbol{\mu}_t^i-\Phi\boldsymbol{\mu}_{t-1}^i\right)\right)^\intercal\boldsymbol{\Sigma}^{-1}\left(z-\Phi\mathbf{P}_{t-1}-\left(\boldsymbol{\mu}_t^i-\Phi\boldsymbol{\mu}_{t-1}^i\right)\right)}\,\mathrm{d}z\,, \tag{8}$$

and

$$\mathbb{P}\left[y_t \in B|I=i\right] = \frac{1}{\sqrt{2\pi\sigma_y^2}}\int_B e^{-\frac{\left(z-\mu_{y,t}^i\right)^2}{2\sigma_y^2}}\,\mathrm{d}z\,, \tag{9}$$

with $\boldsymbol{\Sigma} = \boldsymbol{\sigma}\boldsymbol{\sigma}^\intercal$ the variance-covariance matrix of the risk factors. Thus, conditionally on the information available to the agent, the risk factors and the signal are distributed as a multivariate Gaussian mixture model.

The simulation algorithm described above defines a Markov process $(\mathbf{P}_t, \boldsymbol{\pi}_t)_{t=0,1,\ldots}$.

2.3 Optimal project valuation under scenario uncertainty

Our model is general enough to be applicable in many contexts. In this section, we will focus on two types of investment decisions: (1) an optimal exit problem, where the agent owns a carbon-intensive plant and is considering decommissioning the plant; and (2) an optimal entry problem, where the agent has the option to invest in a green energy project. These problems can be both modeled

as an American option pricing problem, and solved numerically by a Least Squares Monte Carlo (LSMC) approach.

In our model, the agent's incentive to delay the investment decision lies not only in the opportunity to wait for future price information, but also in that of learning about the macroeconomic scenario with greater accuracy. The agent has indeed two main sources of uncertainty: the one stemming from the fluctuations of risk factor values $\mathbf{P}_t$, and the transition scenario uncertainty. This is the main difference with respect to standard real options models, where the value of the underlying only depends on stochastic variables that are commodity prices or other asset prices.

We assume that the agent makes the decision based on the information from the observable risk factor values, and the information about the posterior scenario probabilities deduced from the signal. We thus consider the Markov process $(\mathbf{X}_t := (\mathbf{P}_t, \boldsymbol{\pi}_t))_{t=0,1,\dots}$ defined in the previous section, and denote by $\mathbb{G} = (\mathcal{G}_t)_{t=0,1,\dots}$ the natural filtration of this process.

1. **Optimal exit**
   The problem of an agent who is considering selling (or decommissioning) a potentially stranded asset can be written as the following optimal stopping problem:

$$\sup_{\tau \in \mathcal{T}} \mathbb{E}\left[\sum_{t=1}^{\tau} \beta^t h(\mathbf{P}_t) - \beta^\tau K(\tau)\right], \tag{10}$$

   where $\mathcal{T}$ is the set of $\mathbb{G}$-stopping times with values in $0, 1, 2, \dots, T$, $h(\mathbf{P}_t)$ is the Profit&Loss function of year t, β is a discount factor that accounts both for the time value of money and for the riskiness of the investment, and K is the cost of decommissioning the plant or, when negative, the price at which the plant is sold. At each point in time until the asset's lifetime T, the agent has to decide whether to continue operating the plant or not.

2. **Optimal entry**
   The problem of an agent who is considering a potential investment in a green energy project with lifetime T can be written as the following optimal stopping problem:

$$\sup_{\tau \in \mathcal{T}} \mathbb{E}\left[\sum_{t=\tau}^{\tau+T} \beta^t h(\mathbf{P}_t) - \beta^\tau K(\tau)\right], \tag{11}$$

   where $\mathcal{T}$ is the set of $\mathbb{G}$-stopping times with values in $\mathbb{N}$, $h(\mathbf{P}_t)$ is the profit and loss (P&L) function of year t, β is a discount factor, and K is the capital cost needed to undertake the project. At each point in time, the agent has to decide whether to exercise the real option, or to postpone the decision until more precise information about the potential profitability of the project becomes available.

In what follows, to simplify our presentation, we will focus on case (1), that is the optimal exit problem, with the understanding that our setting fully addresses case (2) as well. Introduce the value function

$$V(t, \mathbf{P}, \hat{\boldsymbol{\pi}}) := \sup_{\tau \in \mathcal{T}_t} \mathbb{E}\left[\sum_{s=t+1}^{\tau} \beta^{(s-t)} h(\mathbf{P}_s) - \beta^{\tau-t} K(\tau) \,\middle|\, (\mathbf{P}_t, \hat{\boldsymbol{\pi}}_t) = (\mathbf{P}, \hat{\boldsymbol{\pi}})\right],$$

where $\mathcal{T}$ is the set of $\mathbb{G}$-stopping times with values in $t, \dots, T$. Note that we use the unnormalized posterior probabilities since they have a simpler dynamics. Normalized probabilities can equivalently be used, with straightforward modifications to the formulas. By standard backward induction

argument, it can be shown that the value function satisfies the following dynamic programming principle:

$$V(t,\mathbf{P},\hat{\boldsymbol{\pi}}) := \max\left\{-K(t), \beta\mathbb{E}\left[h(\mathbf{P}_{t+1}) + V(t+1,\mathbf{P}_{t+1},\hat{\boldsymbol{\pi}}_{t+1}) \,\middle|\, (\mathbf{P}_t,\hat{\boldsymbol{\pi}}_t) = (\mathbf{P},\hat{\boldsymbol{\pi}})\right]\right\} \tag{12}$$

$$= \max\{-K(t), CV\,(t,\mathbf{P}_t,\hat{\boldsymbol{\pi}}_t)\}, \tag{13}$$

where CV is the so called continuation value:

$$CV\,(t,\mathbf{P}_t,\hat{\boldsymbol{\pi}}_t) = \beta\mathbb{E}\left[h(\mathbf{P}_{t+1}) + V(t+1,\mathbf{P}_{t+1},\hat{\boldsymbol{\pi}}_{t+1}) \,\middle|\, \mathbf{P}_t,\hat{\boldsymbol{\pi}}_t\right]. \tag{14}$$

Using the explicit dynamics given in the previous section, this value can be written as follows:

$$CV\,(t,\mathbf{P}_t,\hat{\boldsymbol{\pi}}_t) = \frac{\beta}{\sum_i \hat{\pi}_t^i}\sum_i \hat{\pi}_t^i \frac{1}{\sigma_y\sqrt{|\boldsymbol{\Sigma}|(2\pi)^{K+1}}}\int_{\mathbb{R}^k}\int_{\mathbb{R}} e^{-\frac{1}{2}\left(z-\boldsymbol{\Phi}\mathbf{P}_t-\left(\boldsymbol{\mu}_{t+1}^i-\Phi\boldsymbol{\mu}_t^i\right)\right)^\intercal\boldsymbol{\Sigma}^{-1}\left(z-\Phi\mathbf{P}_t-\left(\boldsymbol{\mu}_{t+1}^i-\Phi\boldsymbol{\mu}_t^i\right)\right)}$$
$$\times\, e^{-\frac{\left(u-\mu_{y,t+1}^i\right)^2}{2\sigma_y^2}}\{h(z) + V(t+1,z,\{\hat{\pi}_t^i e^{-\frac{(u-\mu_{y,t+1}^i)^2}{2\sigma_y^2}}\}_{i=1,\ldots,N})\}\,\mathrm{d}z\,\mathrm{d}u\,.$$

As mentioned, Eq. (12) can be solved numerically by LSMC, that couples backward oriented dynamic programming techniques with forward oriented simulation techniques. The LSMC algorithm works by backward induction, and at each point in time it compares the convenience of immediate exercise with that of delaying the decision. As outlined in [Longstaff and Schwartz, 2001], the continuation value at each possible exercise point can be estimated from a least squares cross-sectional regression using the simulated paths. The algorithm (see Algorithm 1) then returns both the value of the real option V_t and the optimal exercise time τ. In the algorithm, $\tilde{V}_t$ denotes an auxiliary process whose conditional expectation equals the continuation value.

Algorithm 1: Least Squares Monte Carlo

Simulate N_{sim} trajectories of $X_t = [\hat{\pi}_t^1,\cdots,\hat{\pi}_t^N, P_t^1,\cdots,P_t^K]$, for $t = 1,\ldots,T$.
For each trajectory, set $\tilde{V}_T = h(\mathbf{P}_T) - K(T)$;
for $t = T-1:-1:1$ **do**
  Perform a polynomial regression of $Y_t = \beta\tilde{V}_{t+1}$ on X_t;
  Use the result to estimate continuation value CV_t on each trajectory
  if $CV_t + K(t) < 0$ **then**
    exercise is optimal on this trajectory;
    $V_t = -K(t)$ and $\tilde{V}_t = h(\mathbf{P}_t) - K(t)$;
  else
    continuation is optimal on this trajectory;
    $V_t = CV_t$ and $\tilde{V}_t = h(\mathbf{P}_t) + CV_t$
  end
end
$CV_0 = \frac{\beta}{N_{sim}}\sum\tilde{V}_1$;
if $CV_0 + K(0) < 0$ then immediate exercise is optimal and $V_0 = -K(0)$, else $V_0 = CV_0$.

As the algorithm shows, a crucial part in the LSMC procedure is to use the cross-sectional information in the simulation to estimate the expectation on future cash flows. In all the empirical applications that follow, we employ a quadratic specification to regress the discounted value of the payoff at future dates over the simulated state variables. Specifically, our least-squares specification

with which we cross-sectionally regress the continuation values of the different simulated paths j at time t is the following:

$$CV_{t,j} = \alpha_t + \boldsymbol{\vartheta}_t f\left(\hat{\boldsymbol{\pi}}_{t,j}, \mathbf{P}_{t,j}\right) + \varepsilon_{t,j}\,, \tag{15}$$

where $f(\cdot)$ is a second-order polynomial function.

3 Empirical application

3.1 Climate scenarios

Integrated assessment models (IAMs) encompassing feedbacks between the global economy, the energy system and the climate system, are the convenient tool to analyze the economic impacts of climate change and climate change mitigation measures. IAMs are used to generate scenarios of evolution of the economy consistent with given climate objectives, based on a set of assumptions.

In this section, we illustrate how our method can be applied to model transition scenario uncertainty. We employ scenario data from an IAM in the NGFS scenario database[2], namely REMIND-MAGPIE 2.1-4.2. This model is a global multi-regional general equilibrium model with a rather detailed representation of the energy system, belonging to the class of intertemporal optimization models with perfect foresight.

The NGFS scenario database includes 6 alternative scenarios produced with REMIND 2.1 model:

- **Current Policies :** existing climate policies remain in place, and there is no strengthening of ambition level of these policies;
- **Nationally Determined Contributions (NDCs) :** currently pledged unconditional NDCs are implemented fully, and respective targets on energy and emissions in 2025 and 2030 are reached in all countries;
- **Delayed Transition (Disorderly) :** there is a "fossil recovery" from 2020 to 2030; thus this scenario follows the trajectory of the Current Policies scenario until 2030. Only thereafter countries with a clear commitment to a specific net-zero policy target at the end of 2020 are assumed to meet the target, representing regional fragmentation. Regionally fragmented carbon prices converge to a global price near 2070 to keep the 67-percentile of warming below 2°C in 2100, which also allows for temporary overshoot;
- **Below 2°C :** this scenario assumes that optimal carbon prices in line with the long-term targets are implemented immediately after 2020 and keeps the 67-percentile of warming below 2°C throughout the 21st century;
- **Divergent Net Zero (Disorderly) :** optimal carbon prices in line with the long-term targets are implemented immediately after 2020 to bring the median temperature below 1.5°C in 2100, after a limited temporary overshoot. Policy pressure and mitigation efforts are unevenly distributed across sectors;
- **Net Zero 2050 :** global CO_2 emissions are at net-zero in 2050. Furthermore, countries with a clear commitment to a specific net-zero policy target at the end of 2020 are assumed to meet this target.

[2]Release 2.2, available at `https://data.ene.iiasa.ac.at/ngfs/`

From top to bottom, the scenarios display a range of levels of stringency of the climate policy that underlies scenario assumptions. Thus, each scenario entails different paths for the macroeconomic variables in the model, and overall they provide a comprehensive overview of the possible climate states.

3.2 Optimal exit from a carbon-intensive power plant

As a first empirical application, we consider an agent who owns an integrated coal gasification plant with combined cycle, without Carbon Capture and Storage (CCS) technology, and wants to know when it is economically optimal to decommission (or sell) the plant. We assume the cost of decommissioning the plant corresponds to a fraction k of the capital cost of building a new coal gasification power plant, C_C^c. When k is negative, the agent is selling the plant at price $k\,C_C^c$. In the results showcased in Section 3.2.1, we assume $k = 0$, *i.e.* there are no decommissioning costs. A sensitivity analysis for this parameter is shown is Section 3.2.2. The plant is a price taker, and supplies every year a quantity of electricity which depends on the plant's utilization rate (a variable available in each scenario) but not on energy prices. We assume it has a nominal capacity W and it is located in Germany. We further suppose that the plant has a residual lifetime of 30 years, thus, assuming $t_0 = 2020$, we restrict our investment valuation framework to years 2020-2050 of the scenario dataset. Finally, we assume a risk-adjusted discount factor $\beta = e^{-r\Delta t}$, with $r = 1\%$[3]. Because it is not equipped with a CCS filter, the plant has to buy some emission allowances in every period, to comply with an emission trading scheme (ETS). Moreover, in every period, it incurs some operation and maintenance (O&M) costs, both fixed (C_F^c) and proportional to the production output (C_V^c). The production output of the plant depends on the plant utilization rate R_U^c, which equals the ratio of the yearly net electricity production Q^c to the total installed capacity T^c for this specific technology in the selected region. The P&L function of year t of the coal gasification plant, with the appropriate conversion factors, is thus equal to

$$h_t^c = W \cdot R_{Ut}^c \cdot 365.25 \cdot 24 \left(P_{Et} - \frac{P_{Ft}}{R_{Ct}^c} - R_{Et}^c P_{Ct} - C_{Vt}^c \right) - W \cdot C_{Ft}^c, \tag{16}$$

where

$$R_{Ut}^c = \text{Utilization rate} = \frac{Q_t^c}{T_t^c \cdot 365.25 \cdot 24}\,. \tag{17}$$

The variables used and their corresponding unit of measure are listed in Table 1 (we omit the superscript c, indicating the coal gasification technology, to avoid clutter).

The risk factors in this example application, that we model according to (1), are

$$\mathbf{P} = \begin{pmatrix} P_E \\ P_F \\ P_C \end{pmatrix}\,.$$

As mentioned, their mean values $\mu_{\cdot,t}^i$ depend on the scenario i of the chosen scenario dataset, and are given by the corresponding i-th scenario path for that variable. Figure 1 shows how the mean value $\mu_{k,t}^i$ of each risk factor evolves according to scenarios in the REMIND 2.1 model.

The parameters $\mathbf{\Phi}$ and $\boldsymbol{\sigma}$ in (1) are estimated from historical data. Specifically, we use front-month futures data at the monthly frequency from January 2015 to October 2021 of ICE Rotterdam

[3] In Section 3.2.2, we perform a sensitivity analysis relatively to this parameter.

Variables	**Name**	**Units**
Capital costs	C_C	USD2010/kW
O&M costs, fixed	C_F	USD2010/MW/year
O&M costs, variable	C_V	USD2010/MWh
Fuel price	P_F	USD2010/MWh
Conversion efficiency	R_C	per cent
Carbon price	P_C	USD2010/t CO2
Electricity price	P_E	USD2010/MWh
Net electricity production	Q	GWh
Total installed capacity	T	GW
Emission rate	R_E	t CO2/MWh
Plant rated power	W	MW

Table 1: Variables used in the plant evaluation

Coal and of ICE EUA (carbon allowances traded in the EU ETS). For electricity, we employ the average hourly price in the day-ahead market for electricity in Germany traded in the EEX, at the monthly frequency. All data were retrieved using the Macrobond database. Because seasonality is a peculiar stylized fact of electricity prices, we first de-seasonalize our monthly log-price electricity sample with a sinusoidal function accounting for half-yearly and annual seasonality. As for carbon and coal log-prices, we de-trend them by subtracting the annual mean level and a linear trend (see Figure 2). We then estimate a multivariate autoregressive model by maximum likelihood using (de-trended) log-prices. Table 2 shows the resulting estimates for the mean-reversion rates and for the volatility parameters. In the empirical application that follows, we will only employ estimates that are significant at the 95% level, i.e. all entries in the matrix Σ, and all diagonal entries in Φ.

		E	F	C
Φ	E	0.55^{***}	0.02	0.02
		(0.10)	(0.03)	(0.03)
	F	-0.23	0.78^{***}	-0.09
		(0.26)	(0.09)	(0.08)
	C	0.17	0.12	0.38^{***}
		(0.35)	(0.12)	(0.10)
Σ	E	0.17^{***}	0.02^{**}	0.01^{***}
		(0.03)	(0.01)	(0.00)
	F	0.02^{**}	0.02^{***}	0.00^{**}
		(0.01)	(0.01)	(0.00)
	C	0.01^{***}	0.00^{**}	0.02^{***}
		(0.00)	(0.00)	(0.00)

Table 2: Monthly parameter estimates of (1) obtained by estimating a multivariate autoregressive model on de-trended prices of electricity, coal, and carbon. Standard errors are in parenthesis. $^{*} = p < 0.1$, $^{**} = p < 0.05$, $^{***} = p < 0.01$.

To update her beliefs on the climate state, the agent needs to choose which signal to rely on. In this illustration, we assume that the agent chooses the greenhouse gases (GHG) emission level from

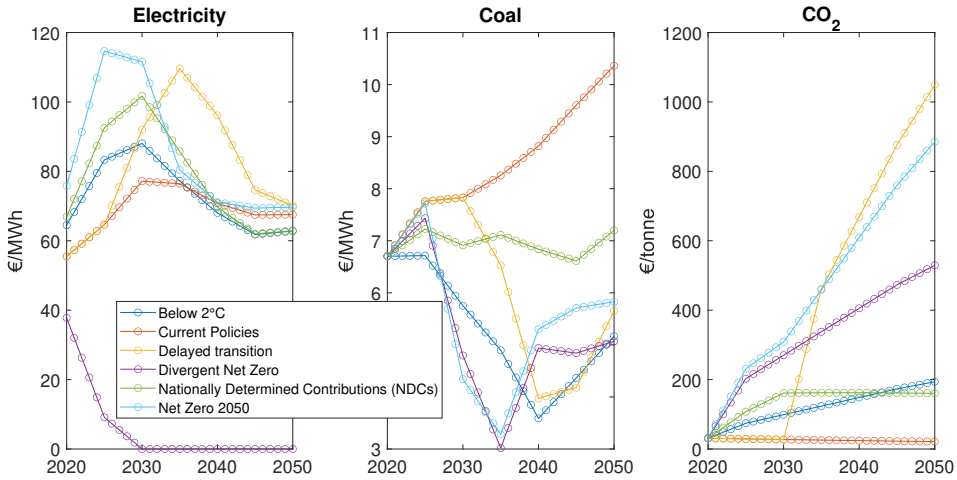

Figure 1: Evolution of the mean value of the three risk factors in the different scenarios produced with the REMIND 2.1 IAM.

energy production in the region where the plant is located (Germany). To estimate the volatility of such a signal y, we use a yearly time series from the Macrobond data set, spanning almost 50 years (from 1970 to 2018), and we fit a Gaussian model. The estimated annual signal volatility parameter is $\hat{\sigma}_y = 108.75$ million tons of CO_2 equivalent. We then employ this value to simulate the signal as in Eq. 2. On the left axis, Figure 3 shows a simulated sample path for the signal y_t (black solid line), when using the scenarios from the REMIND 2.1 model. As the figure shows, after some time, the simulated signal converges towards a specific REMIND 2.1 scenario (in this case scenario 3 – Delayed Transition). The REMIND 2.1 values of the mean GHG emissions path in each scenario are represented by the blue lines. On the right axis, the figure shows the corresponding evolution of the relative conditional probabilities π_t^i, for $i \in \{1, \ldots, 6\}$, computed as in Eq. (6) (red dotted lines, where the tag indicates scenario number). As the signal converges towards scenario $i = 3$, the conditional probability $\pi_t^{i=3}$ gets higher, while all other $\pi_t^{j\neq 3}$ tend to zero.

All variables in Eq. (16) except for the risk factors are modelled as deterministic, and their time-dependent values are extracted from the scenario database, when available. In addition, we assume constant fixed costs C_F^c at 58,000 EUR/MW/year (see [ACIL, 2014]), variable costs C_V^c at 2.6 EUR/MWh, and conversion efficiency R_C^c at 42% (see [IEA, 2012]).

3.2.1 Numerical results

Different scenario datasets may differ not only in the nature of the base assumptions underlying the scenario specifications, but also in the number of scenarios itself. The NGFS REMIND 2.1 dataset offers 6 different scenarios, as discussed in Section 3.1. The ones that matter the most in the context of this empirical application are the ones related to the emissions trajectory, since the signal the agent relies on is closely related to this variable. The span of the paths of this variable in different scenarios represents in a sense the extent to which the agent can decode the state of the system and form a belief about possible implications. It is thus important that the agent has a

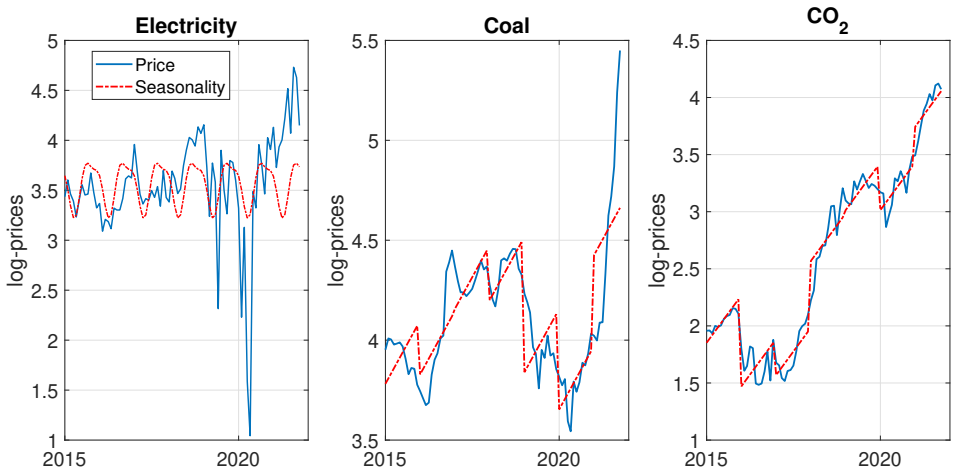

Figure 2: From left to right, EEX day-ahead electricity log-prices in Germany, ICE Rotterdam front-month futures log-prices, ICE EUA front-month futures log-prices (blue lines), and their relative de-trending (red dotted lines).

number of sufficiently diversified scenarios available. To see this, let us analyze two options. First, let us consider the case when an agent has only two available emission scenarios to decode the signal with, and let us suppose that the two are very far apart in their range of values. If scenarios have a range of values much wider than the variability in the signal, the signal, albeit noisy, will likely immediately identify the state of the system, and climate uncertainty would immediately resolve. In this case, the learning process of the agent would end soon, and it would thus not affect much the value of the real option. As a second case, let us consider that the agent has again two available scenarios for the emissions trajectory, very similar one to the other. In this case, because the signal is noisy, it would be very difficult for the agent to decode the state of the system, and to clearly identify which of the two scenarios is the most likely. Thus, the agent would likely assign equal probabilities to the two scenarios. Again, her learning process would not substantially affect her decision making.

Our results confirm this intuition. Indeed, Figure 4 shows the sensitivity in the results of our model to the value of the volatility of the signal in the two cases described above. We let the signal volatility vary in a range $[0; 5\,\hat{\sigma}_y]$. The left panel of the figure depicts the first case, with two divergent scenarios, "Current Policies" and "Net Zero 2050". As Figure 3 shows, these two scenarios entail very different trajectories for the GHG emissions. When the signal volatility is in a range of 0 to 5 times the estimated $\hat{\sigma}_y$, which is not sufficient to cover the range of values spanned by the two scenarios, the value of the project and the optimal exercise time remain constant[4]. The right panel of the figure depicts the second case, with two scenarios that display similar emissions trajectories, "Below 2°C" and "Nationally Determined Contributions (NDCs)". Here, the value of the project is not affected by the volatility of the signal, and the optimal RO exercise time is similarly unaffected.

Figure 5 instead shows the results of our model when all six available scenarios from REMIND

[4]Eventually, as the signal becomes noisier, that is for higher values of σ_y, the value of the project starts to decline.

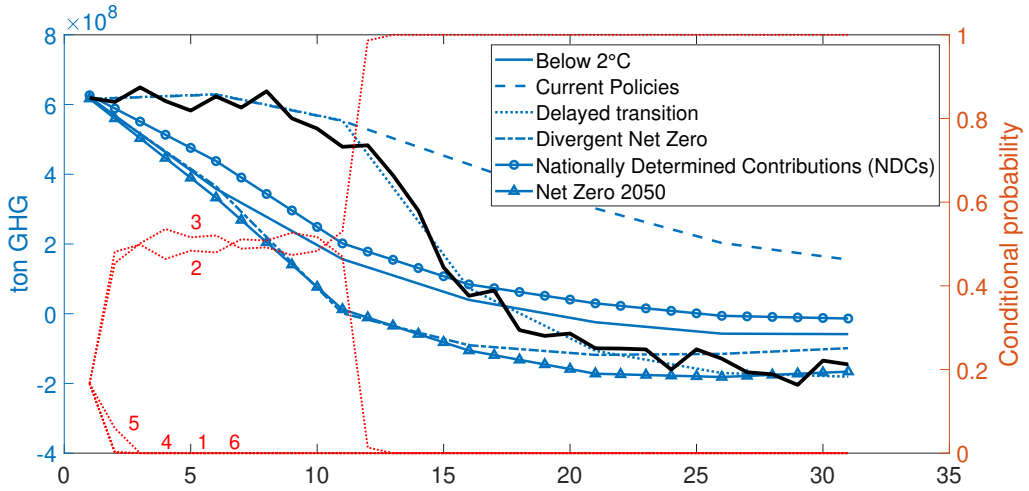

Figure 3: A simulated path for the signal y_t (black solid line), and the relative conditional probabilities π_t^i, for $i \in \{1, \ldots, 6\}$ (red dotted lines; the red tag corresponds to the scenario number i). The blue lines represent the GHG emission trend evolution in each i^{th} scenario according to REMIND 2.1 data.

2.1 are included. In this case, scenarios span a wide range of possible trajectories for the GHG emissions, so that the learning process of the agent has value in her decision making. Indeed, the higher the volatility of the signal, and thus the less precise the signal is in signalling the "true" scenario to the agent, the less valuable the RO. The concave profile of the optimal exercise time reflects the value of information obtained by waiting. When the volatility of the signal is low, the scenario information is quite precise already in the beginning. Then, as the signal volatility increases, it becomes important to observe the signal for a longer time to gather more information about the scenario, so the optimal exercise time increases as well. However, when the volatility of the signal is very high, the value of additional information obtained by waiting is low, thus the optimal stopping time remains constant/decreases slightly. In applications of our model, we recommend using a sufficiently large number of sufficiently diverging scenarios, so as to describe the range of possible futures in a realistic way.

3.2.2 Sensitivity analysis

A crucial parameter in our model is the discount rate reflecting the riskiness of the investment project. Thus, we perform a sensitivity analysis to assess the extent to which our results are affected by the choice of this parameter. Economic intuition commands that lower discount factors β, and thus higher discount rates r, will lead to underweighting future cash flows, and thus to an earlier optimal stopping time τ and to lower values of the project. This is indeed what the right panel of Figure 6 shows, with the project value declining as r increases in the range $[1\%; 10\%]$. This figure also shows the sensitivity to another set of parameters, that is the estimated risk-factors' variance-covariance matrix Σ (left panel). Here, we multiply the estimated variance-covariance matrix by a factor that varies in a range $[\frac{1}{4}; 5]$. When risk factors are more volatile, the flexibility given by

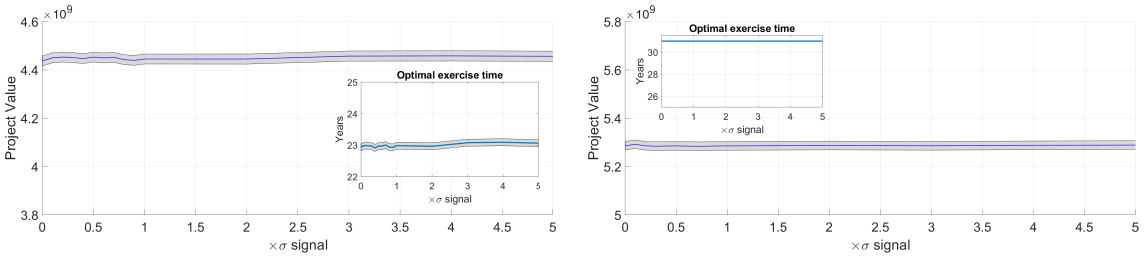

(a) "Current Policies" and "Net Zero 2050" scenarios (b) "Below 2 °C" and "NDCs" scenarios

Figure 4: Optimal exit problem. Sensitivity of the project value (in EUR) to the volatility of the signal, σ_y. In the figure, σ_y varies in a range $[0; 5\,\hat{\sigma}_y]$. In Panel 4a, only scenarios "Current Policies" and "Net Zero 2050" from the REMIND 2.1 are included in the model. In Panel 4b, only scenarios "Below 2°C" and "Nationally Determined Contributions (NDCs)" from the REMIND 2.1 are included. The project value is computed by LSMC with 20,000 simulations, and with a risk-adjusted discount rate $r = 1\%$. The shaded gray area represents the 95% confidence interval. The inset plot shows the sensitivity of the average optimal stopping time τ to the volatility of the signal σ_y, with a 95% confidence interval.

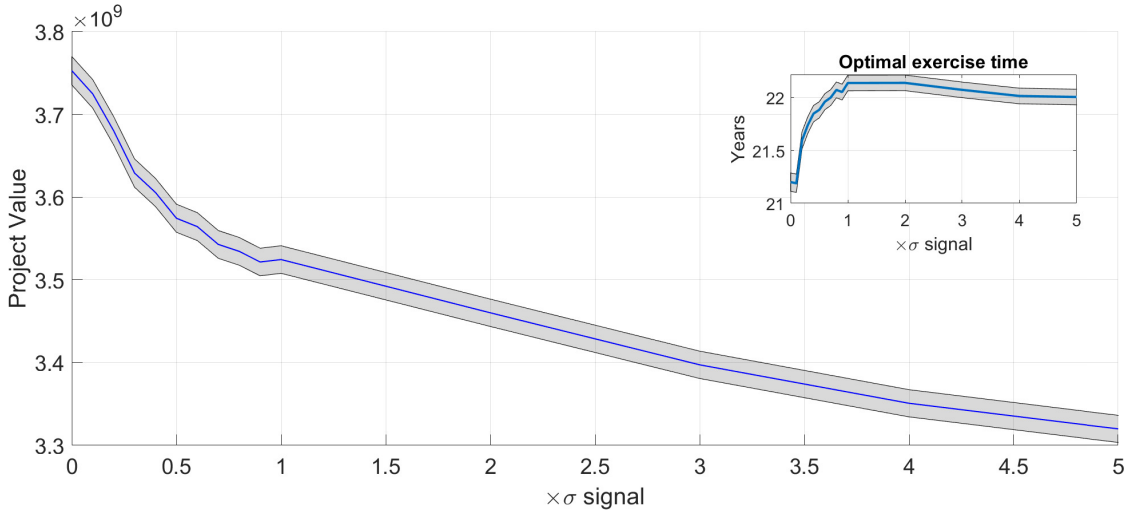

Figure 5: Optimal exit problem. Sensitivity of the project value (in EUR) to the volatility of the signal, σ_y. In the figure, σ_y varies in a range $[0; 10\,\hat{\sigma}_y]$. Here, all available scenarios in REMIND 2.1 are included in the model. The project value is computed by LSMC with 60,000 simulations, and with a risk-adjusted discount rate $r = 1\%$. The shaded gray area represents the 95% confidence interval. The inset plot shows the sensitivity of the average optimal stopping time τ to the volatility of the signal σ_y.

owning the option is more valuable, and the RO value is higher. The uncertainty related to the risk factors leads to postponing the decision, and thus to a higher average optimal exercise time. Finally,

Figure 7 shows that the results showcased in Section 3.2.1 for the sensitivity of both the RO value and the optimal exercise time to the volatility of the signal hold in presence of decommissioning costs or selling revenues. This is true also for both the sensitivity to the risk factors' volatility and the discount factor (figures not shown here). Specifically, the left panel of Figure 7 presents the result in presence of decommissioning costs equal to 10% of the capital costs C_C^c of building a coal gasification plant (at the moment when the option is exercised), while the right panel shows the result in presence of terminal revenues, obtained by selling the plant in τ, equal to 10% of the capital costs C_C^c of building a coal gasification plant.

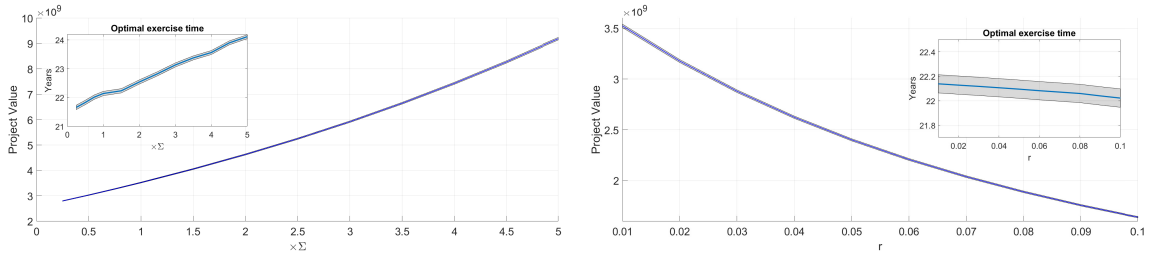

Figure 6: Optimal exit problem. Sensitivity of the project value (in EUR) to the risk factors volatility, Σ (left panel) and to the discount rate r (right panel). In the left panel, Σ varies in a range $[\frac{1}{4}; 5\,\hat{\Sigma}]$, and the project value is computed with a risk-adjusted discount rate $r = 1\%$. All scenarios from REMIND 2.1 dataset are included. The project value is computed by LSMC with 60,000 simulations. The shaded gray area represents the 95% confidence interval. The inset plot shows the sensitivity of the average optimal stopping time τ, with a 95% confidence interval.

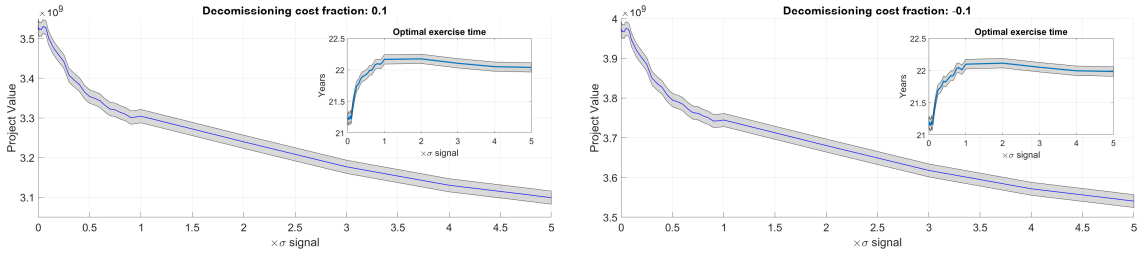

Figure 7: Optimal exit problem. Sensitivity of the project value (in EUR) to the presence of decommissioning costs equal to 10% of the capital costs C_C^c of building a coal gasification plant (left panel) and terminal revenues obtained by selling the plant equal to 10% of the capital costs C_C^c of building a coal gasification plant (right panel). The project value is computed by LSMC with 60,000 simulations, and with a risk-adjusted discount rate $r = 1\%$. All scenarios from the REMIND 2.1 are included. The shaded gray area represents the 95% confidence interval. The inset plot shows the sensitivity of the average optimal stopping time τ, with a 95% confidence interval.

3.3 Optimal entry in a green investment project

As a second empirical application, we consider an agent who has the option to invest in a combined cycle biomass power plant with Carbon Capture and Storage (CCS) technology, and wants to know

when it is economically optimal to exercise the RO. The plant is again a price taker, and will supply electricity inelastically. We assume it has a nominal capacity W and it is located in Germany. We further assume the plant will have a lifespan of 30 years, and we assume $t_0 = 2020$. We set the maturity of the RO at the last available IAM scenario date, that is to 2050 for REMIND 2.1[5]. Finally, we assume a risk-adjusted discount factor $\beta = e^{-r\Delta t}$, with $r = 1\%$. The problem the agent needs to solve is now that of Eq. (11). Exercising the option entails a stream of revenues and costs starting from the exercise time τ throughout the plant lifetime, T. The strike price of the RO corresponds to the capital cost of building a new biomass power plant, C_C^b. Namely, the payoff of the RO at time τ is

$$\max\left(0\,;\sum_{t=\tau}^{\tau+T}\beta^t h^b(\mathbf{P}_t) - C_C^b(\tau)\right).$$

If the agent exercises the option, and thus builds the biomass power plant, in every period t she will incur some output-dependent operation and maintenance (O&M) costs, both fixed (C_F^b) and proportional to the production output (C_V^b). The production output of the plant depends on the plant's utilization rate R_U^b, which equals the ratio of the yearly net electricity production Q^b to the total installed capacity T^b for this specific technology in the selected region. The P&L function of year t of the plant, with the proper conversion factors, is thus equal to

$$h_t^b = W \cdot R_{U\,t}^b \cdot 365.25 \cdot 24 \left(P_{E\,t} - \frac{P_{F\,t}}{R_{C\,t}^b} - C_{V\,t}^b\right) - W \cdot C_{F\,t}^b\,, \tag{18}$$

where

$$R_{U\,t}^b = \text{Utilization rate} = \frac{{Q^b}_t}{{T^b}_t \cdot 365.25 \cdot 24}\,. \tag{19}$$

We refer the reader to Table 1 for the explanation of the remaining variables in Eq. (18), as well as for the variables' units of measure.

The risk factors in this example application, that we model according to (1), are now two:

$$\mathbf{P} = \begin{pmatrix} P_E \\ P_F \end{pmatrix}.$$

Indeed, since the plant is a green investment, it is not required to comply to an ETS, and thus it does not have any carbon-related costs. As before, the risk factors' mean values $\mu_{\cdot,t}^i$ depend on the scenario i of the chosen scenario dataset, and are given by the corresponding i-th scenario path for that variable. Figure 8 shows how the drift $\mu_{k,t}^i$ of each risk factor k evolves according to scenarios in the REMIND 2.1 IAM. The parameters $\boldsymbol{\Phi}$ and $\boldsymbol{\sigma}$ in (1) are estimated from historical data. Specifically, we use front-month futures data at the monthly frequency from January 2015 to October 2021 of CBOT Ethanol to estimate parameters for the biomass power plant fuel. For electricity, we again employ the average hourly price in the day-ahead market for electricity in Germany traded in the EEX, at the monthly frequency. All data were retrieved using the Macrobond database. As in the previous empirical application, we first de-seasonalize our monthly log-price electricity sample with a sinusoidal function accounting for half-yearly and annual seasonality. As for the biofuel log-prices, we de-trend them by subtracting the annual mean level and a linear

[5]If the agent exercises the RO close to the RO maturity, so that the lifespan of the plant goes beyond the latest available IAM scenario date, we assume that the scenario remains constant at the latest available value throughout the residual power plant life.

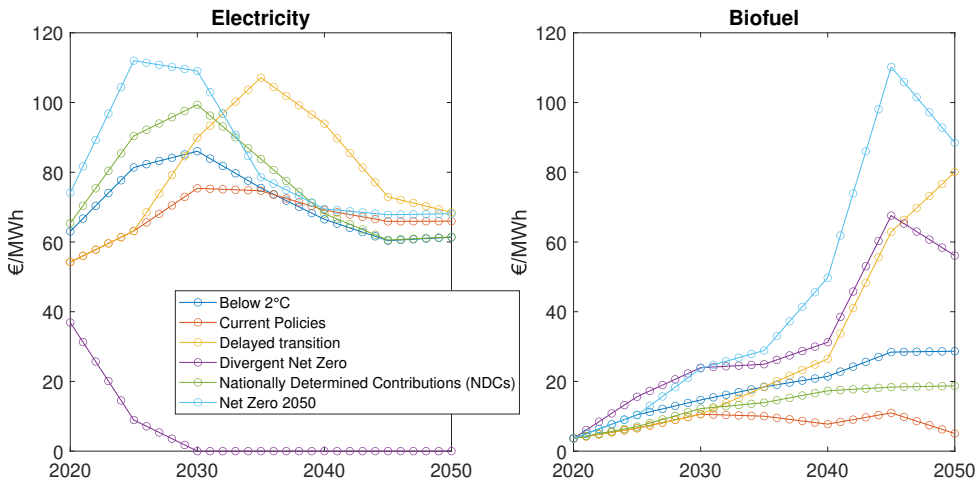

Figure 8: Scenarios, and relative mean risk factor price paths, within the REMIND 2.1 IAM.

trend. We then estimate a multivariate autoregressive model by maximum likelihood using (de-trended) log-prices. Table 3 shows the resulting estimates for the mean-reverting rates and for the volatility parameters. In the empirical application that follows, we will only employ estimates that are significant at the 95% level, i.e. all diagonal entries in both matrices Σ and Φ.

		E	F
Φ	E	0.52***	0.03
		(0.09)	(0.02)
	F	0.80	0.48***
		(0.52)	(0.09)
Σ	E	0.17***	−0.00
		(0.03)	(0.00)
	F	−0.00	0.01***
		(0.00)	(0.00)

Table 3: Monthly parameter estimates of (1) obtained by estimating a multivariate autoregressive model on de-trended electricity and biofuel prices. Standard errors are in parenthesis. $^{*} = p < 0.1$, $^{**} = p < 0.05$, $^{***} = p < 0.01$.

In this case, the agent chooses to use as a signal the price of the EUA. To estimate the volatility of such a signal y, we employ the EEX EUA front-month futures monthly log-prices and we fit a Gaussian model. The estimated monthly signal volatility parameter is $\hat{\sigma}_y = 0.80$. We then employ this value to simulate the signal as in Eq. (2).

All variables in Eq. (18) except for the risk factors are modelled as deterministic, and they follow a trend depending on the availability of scenario trajectories for each one of them. In this case, the REMIND 2.1 model includes scenario paths for the risk factors, for the capital cost C_C^b, that is the strike price of the RO, and for both the total installed capacity of biomass plants (with CCS) T^b

and the electricity production from biomass-fired plant (with CCS) Q^b. This allows the utilization rate R_U^b of the biomass-fired plant to have a scenario-dependent trend. We assume constant fixed costs C_F^b at 81,110 EUR/MW/year, variable costs C_V^b at 10.6 EUR/MWh, and conversion efficiency R_C at 55% (see [IEA, 2017]).

3.3.1 Numerical results

Figure 9 shows the sensitivity of both the RO value and the optimal exercise time to the value of the volatility of the signal for the entry problem, when all six available scenarios from REMIND 2.1 are included. We let the signal volatility vary in a range $[0; 20\,\hat{\sigma}_y]$. Similarly to the previous case, when the signal was the country GHG emission level, scenarios for the carbon price span a wide range of possible trajectories (see Figure 1), so that the learning process of the agent has value in her decision making. Again, the value of the RO is decreasing in the volatility of the signal. Compared to the optimal exit problem, here, with a wider range for the volatility of the signal σ_y, it is evident that when the signal becomes too noisy, there is no value in waiting, and it is actually optimal to exercise the option earlier than in the case when the signal is perfectly revealing the climate state.

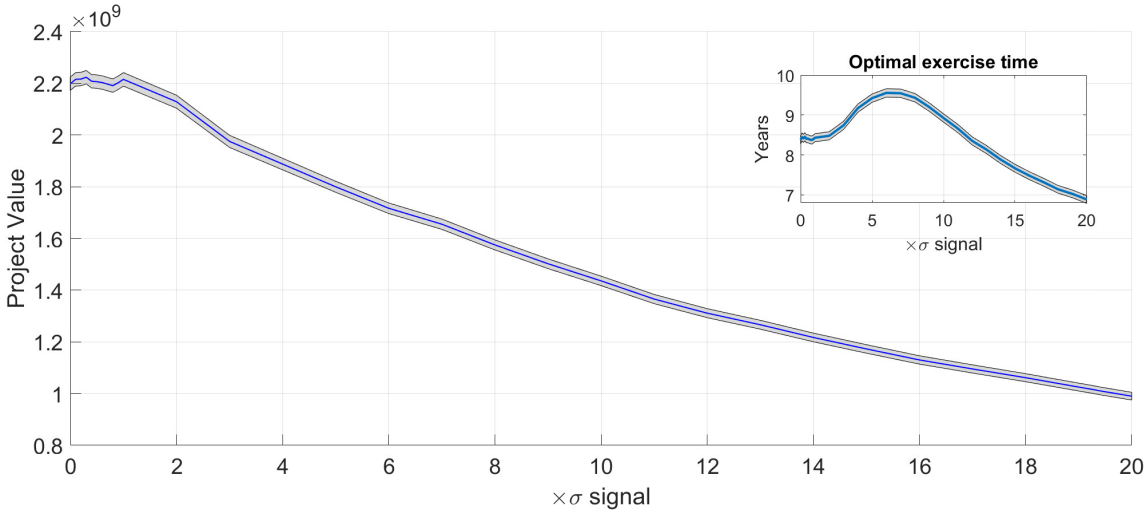

Figure 9: Optimal entry problem. Sensitivity of the project value (in EUR) to the volatility of the signal, σ_y. In the figure, σ_y varies in a range $[0; 20\,\hat{\sigma}_y]$. Here, all available scenarios in REMIND 2.1 are included in the model. The project value is computed by LSMC with 60,000 simulations, and with a risk-adjusted discount rate $r = 1\%$. The shaded gray area represents the 95% confidence interval. The inset plot shows the sensitivity of the average optimal stopping time τ to the volatility of the signal σ_y.

Figure 10 shows the sensitivity of the RO value and of the average optimal stopping time to both the volatility of the risk factors Σ (left panel) and the discount rate r (right panel). We let r vary in a range $[1\%; 10\%]$, and we multiply the estimated variance-covariance matrix by a factor that varies in a range $[\frac{1}{4}; 5]$. As in the optimal exit problem, the RO value is increasing in the volatility of the risk factors and decreasing in the discount rate. However, here, the average optimal exercise

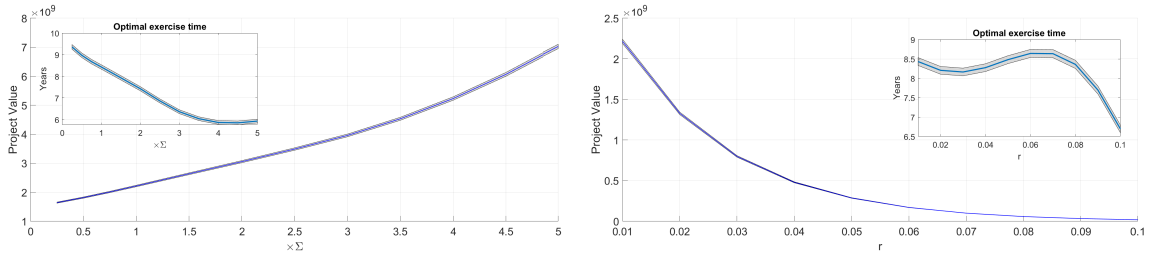

Figure 10: Optimal entry problem. Sensitivity of the project value (in EUR) to the risk factors volatility, Σ (left panel) and to the discount rate r (right panel). In the left panel, Σ varies in a range $[\frac{1}{4}; 5\,\hat{\Sigma}]$, and the project value is computed with a risk-adjusted discount rate $r = 1\%$. All scenarios from the REMIND 2.1 are included. The project value is computed by LSMC with 60,000 simulations. The shaded gray area represents the 95% confidence interval. The inset plot shows the sensitivity of the average optimal stopping time τ, with a 95% confidence interval.

time is decreasing in the volatility of the risk factors. Thus, the higher the variability relative of the future cash flows, the earlier it is convenient to invest in the green energy project.

4 Conclusions

In this paper, we present a new strategy for evaluating investment projects, by combining standard real options techniques with a macroeconomic approach for climate transition analysis. In our model, the agent continuously observes a noisy climate-related signal, and forms a belief relative to the likelihood of the current macroeconomic climate scenario. The agent then bases her entry or exit decisions on the posterior probability of being in a certain macroeconomic scenario. The agent's learning about the level of climate risk, via Bayesian updating, then plays an active role in the decision making process.

We showcase the potential of our strategy using public available scenario data from the NGFS scenario database, which are representative of a range of several different environmental transition pathways. Each of them is associated to a certain level of climate policy stringency, from low (existing climate policies remain in place, with no further effort to mitigate climate change), to high (there is a clear commitment to a specific net-zero policy target that results in CO_2 emissions to be at net-zero in 2050).

Our results indicate that taking into account scenario uncertainty and its progressive resolution is essential for precise valuation of energy projects. Furthermore, they underscore the importance of reliable and detailed climate scenarios. In particular, the IAM we adopt in the empirical application section of this paper is not designed to simulate structural changes. Moreover, features like higher time granularity and increased geographical diversity would add precision to our results. Finally, for the purpose of energy project valuation, it would be important to have an IAM that includes energy producer-specific variables, such as the wholesale price of electricity at the primary level, rather than at the secondary one (which also includes dispatching costs).

References

[Abadie et al., 2011] Abadie, L. M., Chamorro, M., González-Eguino, M., et al. (2011). Optimal abandonment of eu coal-fired stations. *The Energy Journal*, 32(3).

[ACIL, 2014] ACIL (2014). Fuel and technology cost review – report to australian energy market operator.

[Bogdanov et al., 2019] Bogdanov, D., Farfan, J., Sadovskaia, K., Aghahosseini, A., Child, M., Gulagi, A., Oyewo, A. S., Barbosa, L. d. S. N. S., and Breyer, C. (2019). Radical transformation pathway towards sustainable electricity via evolutionary steps. *Nature communications*, 10(1):1–16.

[Boomsma et al., 2012] Boomsma, T. K., Meade, N., and Fleten, S.-E. (2012). Renewable energy investments under different support schemes: A real options approach. *European Journal of Operational Research*, 220(1):225–237.

[Cronin et al., 2018] Cronin, J., Anandarajah, G., and Dessens, O. (2018). Climate change impacts on the energy system: a review of trends and gaps. *Climatic change*, 151(2):79–93.

[Dalby et al., 2018] Dalby, P. A., Gillerhaugen, G. R., Hagspiel, V., Leth-Olsen, T., and Thijssen, J. J. (2018). Green investment under policy uncertainty and Bayesian learning. *Energy*, 161:1262–1281.

[Detemple and Kitapbayev, 2020] Detemple, J. and Kitapbayev, Y. (2020). The value of green energy: Optimal investment in mutually exclusive projects and operating leverage. *The Review of Financial Studies*, 33(7):3307–3347.

[Flora and Vargiolu, 2020] Flora, M. and Vargiolu, T. (2020). Price dynamics in the European Union Emissions Trading System and evaluation of its ability to boost emission-related investment decisions. *European Journal of Operational Research*, 280(1):383–394.

[Fuss et al., 2012] Fuss, S., Szolgayová, J., Khabarov, N., and Obersteiner, M. (2012). Renewables and climate change mitigation: Irreversible energy investment under uncertainty and portfolio effects. *Energy Policy*, 40:59–68.

[Hach and Spinler, 2016] Hach, D. and Spinler, S. (2016). Capacity payment impact on gas-fired generation investments under rising renewable feed-in—a real options analysis. *Energy Economics*, 53:270–280.

[IEA, 2012] IEA (2012). Technology roadmap - high-efficiency, low-emissions coal-fired power generation.

[IEA, 2017] IEA (2017). Technology roadmap - delivering sustainable bioenergy.

[Laurikka and Koljonen, 2006] Laurikka, H. and Koljonen, T. (2006). Emissions trading and investment decisions in the power sector—a case study in finland. *Energy Policy*, 34(9):1063–1074.

[Longstaff and Schwartz, 2001] Longstaff, F. A. and Schwartz, E. S. (2001). Valuing american options by simulation: a simple least-squares approach. *The Review of Financial Studies*, 14(1):113–147.

[McGlade and Ekins, 2015] McGlade, C. and Ekins, P. (2015). The geographical distribution of fossil fuels unused when limiting global warming to 2 c. *Nature*, 517(7533):187–190.

[Mercure et al., 2018] Mercure, J.-F., Pollitt, H., Viñuales, J. E., Edwards, N. R., Holden, P. B., Chewpreecha, U., Salas, P., Sognnaes, I., Lam, A., and Knobloch, F. (2018). Macroeconomic impact of stranded fossil fuel assets. *Nature Climate Change*, 8(7):588–593.

[Mo et al., 2021] Mo, J., Cui, L., and Duan, H. (2021). Quantifying the implied risk for newly-built coal plant to become stranded asset by carbon pricing. *Energy Economics*, 99:105286.

[Rozenberg et al., 2020] Rozenberg, J., Vogt-Schilb, A., and Hallegatte, S. (2020). Instrument choice and stranded assets in the transition to clean capital. *Journal of Environmental Economics and Management*, 100:102183.

[Siddiqui and Fleten, 2010] Siddiqui, A. and Fleten, S.-E. (2010). How to proceed with competing alternative energy technologies: A real options analysis. *Energy Economics*, 32(4):817–830.

[Stanton et al., 2016] Stanton, M. C. B., Dessai, S., and Paavola, J. (2016). A systematic review of the impacts of climate variability and change on electricity systems in europe. *Energy*, 109:1148–1159.

[Teske, 2019] Teske, S. (2019). *Achieving the Paris climate agreement goals: global and regional 100% Renewable energy scenarios with non-energy GHG pathways for+ 1.5 C and+ 2 C*. Springer Nature.

[van der Ploeg and Rezai, 2020] van der Ploeg, F. and Rezai, A. (2020). The risk of policy tipping and stranded carbon assets. *Journal of Environmental Economics and Management*, 100:102258.

[Welsby et al., 2021] Welsby, D., Price, J., Pye, S., and Ekins, P. (2021). Unextractable fossil fuels in a 1.5 c world. *Nature*, 597(7875):230–234.